On Time-Synchronized Stability and Control

Dongyu Li, Haoyong Yu, Keng Peng Tee, Yan Wu, Shuzhi Sam Ge, and Tong Heng Lee

***Abstract*—Previous research on finite-time control focuses on forcing a system state (vector) to converge within a certain time moment, regardless of how each state element converges. In the present work, we introduce a control problem with unique finite/fixed-time stability considerations, namely *time-synchronized stability*, where *at the same time*, all the system state elements converge to the origin, and *fixed-time-synchronized stability*, where the upper bound of the synchronized settling time is invariant with any initial state. Accordingly, sufficient conditions for (fixed-) time-synchronized stability are presented. On the basis of these formulations of the time-synchronized convergence property, the classical sign function, and also a *norm-normalized sign function*, are first revisited. Then in terms of this notion of time-synchronized stability, we investigate their differences with applications in control system design for first-order systems (to illustrate the key concepts and outcomes), paying special attention to their convergence performance. It is found that while both these sign functions contribute to system stability, nevertheless an important result can be drawn that norm-normalized sign functions help a system to additionally achieve time-synchronized stability. Further, we propose a fixed-time-synchronized sliding-mode controller for second-order systems; and we also consider the important related matters of singularity avoidance there. Finally, numerical simulations are conducted to present the (fixed-) time-synchronized features attained; and further explorations of the merits of the proposed (fixed-) time-synchronized stability are described.**

***Index Terms*—Time-synchronized convergence, sliding-mode control, Lyapunov analysis.**

I. Introduction

DUE to the great potential for high-precision performance of finite-time control design, it has become an active development topic with wide applications in various interesting areas, such as attitude stabilization of spacecraft [1]–[3], trajectory tracking of robotic manipulators [4]–[6], cooperative control of multi-agent systems [7]–[10], state estimation of dynamical systems [11]–[13], *etc*. In general, finite-time stabilization guarantees finite-time convergence of the system state [14], where more specifically, before a certain time moment, all the system state elements arrive at the origin. Further, it can be noted that such related fixed-time stability was proposed in [15] to predefine guaranteed settling time of the closed-loop system, regardless of the initial conditions. For some classes of practical systems, unfortunately, standalone finite- or fixed-time convergence is not enough during certain operations, in which the control system (with diversified subsystems) is expected to accomplish multiple actions synchronously (the state elements converge to desired values at the same time). For example, the finger joints of a robotic hand may be required to reach the desired angles synchronously in order to grasp an object firmly. For multi-agent missions, the networked systems are generally required to likewise synchronously reach a target (*e.g.*, cooperative missile attacks [16]).

Motivated by the above observation, we investigate unique types of finite/fixed-time stability formulations — *time-synchronized stability* (TSS) and *fixed-time-synchronized stability* (FTSS), where all the system state elements converge to the origin at the same time, with the estimation of the synchronized settling time variant/invariant with the initial state. It is noteworthy that TSS has already been conceptualized in our previous work [17]. Nevertheless, the specific definitions, the stability formulations, and the corresponding control design based on TSS are not yet explored in detail. Further, the concept of FTSS has not been touched on.

To solve this problem, the properties of sign functions are first explored that are widely utilized in control system design, industrial electronics, and signal processing [18]–[27]. Especially for sliding-mode control, the sign function provides robustness against matched disturbances [28]–[30], and it is one of the most commonly used mathematical tools to design a finite/fixed-time control law. In particular, two distinct types of multi-variable sign functions, *i.e.*, the *classical sign function* and the *norm-normalized (NN) sign function* are revisited, as well as their influence on the control effect. This latter function is also described and called as the *unit vector* in [31]–[33], but there, while some examples of effectiveness were shown, the detailed different contributions of the two functions to the system stability and convergence were then not deeply explored nor fully developed. The classical sign function is usually referred to as the sign function or the signum function, extracting the sign of any real numbers. The NN sign function gets its name because, while generally rather similar to the classical sign function, it additionally utilizes the normalization of the input vector (and thus yielding inherently different and rather important properties). In the literature, most existing results on control systems use the classical sign function to design a controller for single-input single-output systems, and the NN sign function for multi-input multi-output systems. However, despite the abundant results on the NN sign function (*e.g.*, in [31]–[35], the NN sign functions are employed to simplify the sliding-mode control design for multi-input and Lagrangian systems), (fixed-) time-synchronized stability on the basis of the NN sign function have not been explored.

Our aim here is to show the different features of the two sign functions in the following sense: (i) in terms of control design,

This work was supported by the Science and Engineering Research Council, Agency of Science, Technology and Research, Singapore, through the National Robotics Program under Grant No. 192 25 00054. Dongyu Li is with the School of Cyber Science and Technology, Beihang University, Beijing 100191, China. Dongyu Li and Haoyong Yu are also with the Department of Biomedical Engineering, National University of Singapore, Singapore 117583, Singapore. Keng Peng Tee and Yan Wu are with the Institute for Infocomm Research, A*STAR, Singapore 138632. Shuzhi Sam Ge and Tong Heng Lee are with the Department of Electrical and Computer Engineering, National University of Singapore, Singapore 117583, Singapore. (corresponding author: bieyhy@nus.edu.sg).

both functions can be applied to design general controllers, such as finite/fixed-time control, sliding-mode control, etc; and (ii) the NN sign function has superior performance, guiding the closed-loop system to additionally achieve these newer notions and outcomes of TSS or FTSS. The key novel embedded attribute lies in that, considering an input vector of dimension n, n individual scalars are generated by classical sign functions, while NN sign functions incorporate the normalization computation of the input vector with its norm. From a qualitative aspect, each output element of NN sign functions contains information of the whole input vector, while the classical sign function does not. Therefore, noting this key embedded attribute, it is thus not unexpected that the more stringent outcomes of (F)TSS are generally not possible to be expected from the classical sign function; but now certainly evidently possible from the NN sign function because it is tightly coupled together with all the elements of its input vector.

This approach holds the following contributions. Firstly, (fixed-) time-synchronized control problems are presented, and we formally introduce definitions of TSS and FTSS. A system is called time-synchronized stable (abbreviated also as TSS) if all the closed-loop system state elements reach the equilibrium at the same time; and called fixed-time-synchronized stable (FTSS) if it is TSS and additionally with the synchronized settling time's upper bound independent of the initial state. Consequently, these notions of TSS and FTSS could be treated as special kinds of finite/fixed-time stability as they already meet the requirements of finite/fixed-time stability. This also provides a theoretical foundation for a very recent approach on (fixed-) time-synchronized consensus [36], where consensus is achieved by network systems at the same time.

Secondly, to further articulate the time-synchronized convergence property, the concept of *ratio persistence* is defined. The solution of a system is ratio persistent if the ratio of the closed-loop state elements is time-invariant in forward time. The ratio persistent property serves as the basis of achievement of time-synchronized convergence. This property is also capable of enhancing the system performance by yielding a shorter and smoother output trajectory, *e.g.*, in the 2- and 3-dimensional space, the trajectory of a ratio persistent system state is a straight line. Given these developments and characterizations of ratio persistence and the NN sign function, we propose, based on Lyapunov functions, two relevant Lyapunov-type theorems for TSS and FTSS, respectively. These theorems provide sufficient conditions to prove TSS and FTSS, and offer a constructive guide to a suitable (fixed-) time-synchronized controller, *i.e.*, "*Fixed/Finite-Time Stability*" + "*Ratio Persistence*" $\Rightarrow$ "*(Fixed-) Time-Synchronized Stability*". The present paper is the first regular publication of these Lyapunov stability results with corresponding proofs.

Thirdly, according to the introduced Lyapunov conditions, we design a time-synchronized control (TSC) law for a class of first-order systems as a starting point to reveal the nature of TSS, in comparison with a finite-time controller. The merit of the NN sign function compared with the classical sign function is also elaborated. Next, based on FTSS, we propose (directly) a non-singular fixed-time-synchronized control (FTSC) algorithm. Actually, as a pertinent aside, it can be noted that for finite/fixed-time control using classical sign functions, the singularity-avoidance issue was addressed with a variety of techniques (refer to the elegant non-singular controllers in [37]–[45]). Here, in virtue of the NN sign function, a series of control laws for first-order and for second-order systems have been proposed and proved to be (fixed-) time-synchronized stable. Moreover, the controller proposed here for second-order systems is directly singularity-free; and this extension is certainly non-trivial, as the otherwise state of the art modification schemes (as mentioned above) which would have been required to avoid a singularity (when only the classical sign function is employed) cannot be directly applied.

Lastly (but certainly not least), this approach is also of practical contributions, as the performance of many real-world systems depends largely on how and when the state of the closed-loop system converges. For example, we usually require all the state elements of artificial satellites, unmanned aerial vehicles, space manipulators, *etc*., to reach a desired state at the same time during their re-pointing/maneuver/on-orbit operations.

The remainder of this approach can be summarized as follows. In Section II, the properties of the classical sign function and the NN sign function are briefly introduced. In Section III, TSS and FTSS, as well as their related Lyapunov conditions are described, based on which a series of controllers are designed for first-order systems and second-order systems. Simulations are presented in Section IV to showcase the merit of (F)TSC. Pertinent conclusions are provided in Section V.

Notations: Let $\mathbb{R}$ denote the set of real numbers, and $I_n \in \mathbb{R}^{n\times n}$ the n-dimensional identity matrix. Let $\lambda_{\max}(\cdot)$ and $\lambda_{\min}(\cdot)$ denote the maximum and minimum eigenvalues of a matrix, respectively. Denote $\operatorname{diag}(x_1,\ldots,x_n) \in \mathbb{R}^{n\times n}$ as the diagonal matrix with diagonal entries $x_1,\ldots,x_n$. Denote $\|\cdot\|$ as the L_2-norm of a vector.

II. Preliminaries and Problem Formulations

Before further proceeding, we list the following abbreviations in Table I.

TABLE I
Abbreviations

Abbreviations	Meanings
NN	Norm-Normalized
(F)TSC	(Fixed-) Time-Synchronized Control
(F)TSS	(Fixed-) Time-Synchronized Stability/Stable

A. Sign Functions

The classical sign function $\operatorname{sign}_{\mathrm{c}}$ and the NN sign function $\operatorname{sign}_{\mathrm{n}}$ are first introduced

$$\operatorname{sign}_{\mathrm{c}}(x) \triangleq [\operatorname{sgn}(x_1),\ \operatorname{sgn}(x_2),\ldots,\ \operatorname{sgn}(x_n)]^T, \quad (1)$$

$$\operatorname{sign}_{\mathrm{n}}(x) \triangleq \begin{cases} \frac{x}{\|x\|}, & x \neq 0, \\ 0, & x = 0, \end{cases} \quad (2)$$

where $x = [x_1,\ x_2, \ldots,\ x_n]^T \in \mathbb{R}^n$, and

$$\operatorname{sgn}(x_i) \triangleq \begin{cases} +1, & x_i > 0, \\ 0, & x_i = 0, \\ -1, & x_i < 0, \end{cases} \tag{3}$$

with $i = 1, 2, \ldots, n$.

In particular, $\operatorname{sign}_{\mathrm{c}}(x)$ maps all vectors from the same orthant into one vector, while $\operatorname{sign}_{\mathrm{n}}(x)$ maps all vectors into the directions of themselves. An illustrated example is shown in Fig. 1, where the red arrow denotes $\operatorname{sign}_{\mathrm{n}}(x)$ and the blue arrow $\operatorname{sign}_{\mathrm{c}}(x)$.

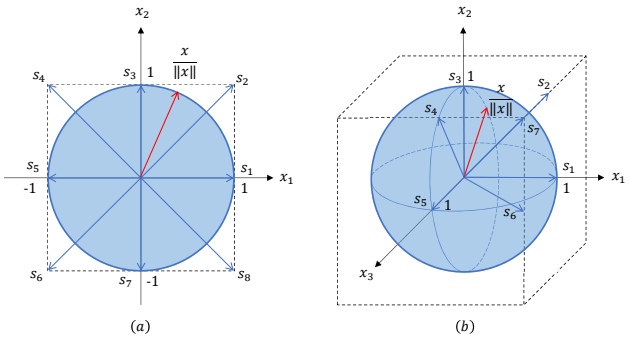

(a) 2-D example (b) 3-D example

Fig. 1. $\operatorname{sign}_{\mathrm{c}}(x)$ and $\operatorname{sign}_{\mathrm{n}}(x)$ in 2-D and 3-D.

We now give the relation between $\operatorname{sign}_{\mathrm{c}}(x)$ and $\operatorname{sign}_{\mathrm{n}}(x)$. (While these properties have been previously addressed in [17], we provide them here for completeness.)

i $\operatorname{sign}_{\mathrm{c}}(x) = \operatorname{sign}_{\mathrm{n}}(x)$ iff $x = 0$ or x contains only one non-zero element while the others (if $n \geq 2$) are all zero. Otherwise, $\operatorname{sign}_{\mathrm{c}}(x) \neq \operatorname{sign}_{\mathrm{n}}(x)$.

ii $\|\operatorname{sign}_{\mathrm{c}}(x)\| \leq \sqrt{n}$, while $\|\operatorname{sign}_{\mathrm{n}}(x)\| = 1$ if $x \neq 0$.

iii $x^T \operatorname{sign}_{\mathrm{c}}(x) = \sum_{i=1}^{n} |x_i| = \|x\|_1$, while $x^T \operatorname{sign}_{\mathrm{n}}(x) = \|x\|^2/\|x\| = \|x\|$.

iv Consider a positive (negative) definite matrix $A \in \mathbb{R}^{n\times n}$. For $x \neq 0$, $x^T A \operatorname{sign}_{\mathrm{n}}(x)$ is positive (negative) definite as $x^T A \operatorname{sign}_{\mathrm{n}}(x) = x^T A\, x/\|x\|$, while in general, $x^T A \operatorname{sign}_{\mathrm{c}}(x)$ does not hold the same property.

Further, based on $\operatorname{sign}_{\mathrm{c}}$ and $\operatorname{sign}_{\mathrm{n}}$, the following continuous modifications are proposed, offering more freedom to control design due to an adjustable power α,

$$\operatorname{sig}_{\mathrm{c}}^{\alpha}(x) = [\operatorname{sign}_{\mathrm{c}}(x_1)\,|x_1|^{\alpha}, \ldots, \operatorname{sign}_{\mathrm{c}}(x_n)\,|x_n|^{\alpha}]^T, \tag{4}$$

$$\operatorname{sig}_{\mathrm{n}}^{\alpha}(x) = \|x\|^{\alpha} \operatorname{sign}_{\mathrm{n}}(x), \tag{5}$$

where $\operatorname{sig}_{\mathrm{c}}^{\alpha}(x)$ and $\operatorname{sig}_{\mathrm{n}}^{\alpha}(x)$ are continuous, and α is usually selected as a positive constant.

We next provide some useful properties of $\operatorname{sig}_{\mathrm{n}}^{\alpha}(x)$.

Lemma 1: [36] For any real vector $x \in \mathbb{R}^n$,

$$\frac{\partial}{\partial x}\|x\|^{\alpha+1} = (\alpha+1)\,\|x\|^{\alpha-1} x, \tag{6}$$

$$\frac{\mathrm{d}}{\mathrm{d}t}\|x\|^{\alpha+1} = (\alpha+1)\,\|x\|^{\alpha-1} x^T \dot{x}, \tag{7}$$

$$\frac{\partial}{\partial x}\operatorname{sig}_{\mathrm{n}}(x)^{\alpha+1} = \alpha\|x\|^{\alpha-2} x x^T + \|x\|^{\alpha} I_n. \tag{8}$$

Lemma 2: [36] Consider a vector

$$z = [z_1^T, z_2^T, \ldots, z_N^T]^T \in \mathbb{R}^{Nn},\ z_i \in \mathbb{R}^n,\ i = 1, 2, ..., N,$$

where N and n are positive integers. Each element of $[\operatorname{sign}_{\mathrm{n}}(z_1)^T, \operatorname{sign}_{\mathrm{n}}(z_2)^T, \ldots, \operatorname{sign}_{\mathrm{n}}(z_N)^T]^T$ is greater than or equal to the corresponding element of $\operatorname{sign}_{\mathrm{n}}(z)$. For convenience, we denote it as

$$\left[\operatorname{sign}_{\mathrm{n}}(z_1)^T, \operatorname{sign}_{\mathrm{n}}(z_2)^T, \ldots, \operatorname{sign}_{\mathrm{n}}(z_N)^T\right]^T \dot{\geq} \operatorname{sign}_{\mathrm{n}}(z).$$

Lemma 3: For a vector $x \in \mathbb{R}^n$, and constants $\alpha > 0$ and $\beta > 0$,

$$\|x\|^{\alpha-\beta} x x^T \operatorname{sig}_{\mathrm{n}}^{\alpha}(x) = \operatorname{sig}_{\mathrm{n}}^{2\alpha-\beta+2}(x). \tag{9}$$

Proof: From (5),

$$\|x\|^{\alpha-\beta} x x^T \operatorname{sig}_{\mathrm{n}}^{\alpha}(x) = \|x\|^{2\alpha-\beta} x x^T \operatorname{sign}_{\mathrm{n}}(x). \tag{10}$$

By element-wisely analyzing $x x^T \operatorname{sign}_{\mathrm{n}}(x)$ in the case of $x = 0$ and the case of $x \neq 0$, we have

$$x x^T \operatorname{sign}_{\mathrm{n}}(x) = \operatorname{sig}_{\mathrm{n}}^{2}(x). \tag{11}$$

Taking (11) into (10) results in (9). ■

B. Other Technical Lemmas

The system dynamics is given as follows,

$$\dot{x} = f(x),\ f(0) = 0,\ x(0) = x_0, \tag{12}$$

where considering an open neighborhood $\mathcal{D}_0 \subseteq \mathbb{R}^n$ of the origin, $f : \mathcal{D}_0 \to \mathbb{R}^n$ is continuous, and there exist a unique solution for any initial state of the system (12) in forward time.

Next, we introduce well-established results on finite/fixed-time stability.

Lemma 4: [46] Considering the system (12), for any real numbers $c > 0$ and $\alpha \in (0, 1)$, the origin of a Lyapunov function $V(x)$ is finite-time stable if

$$\dot{V}(x) + cV^{\alpha}(x) \leq 0, \tag{13}$$

where the settling time is estimated by

$$T(x_0) \leq \frac{V^{1-\alpha}(x_0)}{c(1-\alpha)}, \tag{14}$$

with the initial value x_0.

Lemma 5: [15] The system (12) is fixed-time stable, if for a radially unbounded Lyapunov function $V(x)$, we have

$$\dot{V}(x) \leq -\left(\alpha V^{p}(x) + \beta V^{g}(x)\right)^{\chi}, \tag{15}$$

where α, β, p, g and χ are positive constants, satisfying $p\chi < 1$ and $g\chi > 1$. The settling time T is bounded as

$$T \leq \frac{1}{\alpha^{\chi}(1-p\chi)} + \frac{1}{\beta^{\chi}(g\chi-1)}. \tag{16}$$

III. Main Results

In this section, TSS and FTSS with relevant Lyapunov-like theorems are proposed, and a series of controllers are properly designed for first-order systems and second-order systems to achieve the proposed stability results.

A. Time-Synchronized Stability

We here formally define TSS.

Definition 1: (*Time-Synchronized Stability*). The equilibrium of the system (12) is *time-synchronized stable* if

i. it is finite-time stable;

ii. for an open neighborhood $\mathcal{N}_0 \subseteq \mathcal{D}_0$ of the origin, there exists a function $T : \mathcal{N}_0 \backslash \{0\} \to (0, \infty)$, called the *synchronized settling-time function*, such that for $\forall x_0 \in \mathcal{N}_0 \backslash \{0\}$ and $i \in \{1, 2, \ldots, n\}$, we have $x(t) \in \mathcal{N}_0$, $\forall t \in [0, \infty)$, and for $x_i(0) \neq 0$,

$$x_i(t) \neq 0, \ \lim_{t \uparrow T(x_0)} x_i(t) = 0, \ \forall t \in [0, T(x_0)), \tag{17}$$

where $T(x_0)$ is the *synchronized settling time*.

The equilibrium of the system (12) is *globally time-synchronized stable* if it is time-synchronized stable with $\mathcal{N}_0 = \mathcal{D}_0 = \mathbb{R}^n$.

According to Definition 1, TSS is a unique type of finite-time stability, as TSS already meets its definition and requirement. Note that there exist several slightly different definitions of finite-time stability (e.g., definitions in [46], [47]), which is not the focus of this paper. Intuitively, one of the techniques to achieve TSS is to guarantee that: (i) the system (12) is finite-time stable; and (ii) during the convergence, the ratio of each pair of the state elements is a constant. Since all the state elements converge to the equilibrium simultaneously, the above two conditions sufficiently lead to TSS, which further motivates the following notion.

Definition 2: (*Ratio Persistence*). The closed-loop state x of the system (12) is *ratio persistent* if for $x \neq 0$, we have

$$\frac{x}{\|x\|} = \zeta \frac{f(x)}{\|f(x)\|}, \tag{18}$$

where ζ is the *direction of ratio persistence*, which can be either 1 or -1.

The condition of ratio persistence seems to be strict, while in fact, numerous control laws in the literature have the potential to force the closed-loop system to achieve the ratio persistence, especially for those where a unit vector is utilized, to name a few, the control design in [31], [33]–[35], [48]–[50].

From Definition 2, a ratio persistent state x satisfies $\dot{x} = \kappa(x) x$, where the function $\kappa : \mathcal{N}_0 \backslash \{0\} \to \mathbb{R}$ is defined as

$$\kappa(x) = \zeta^{-1} \frac{\|f(x)\|}{\|x\|}. \tag{19}$$

From (18), we know $\kappa(x) \neq 0$ when $x \neq 0$. Next, for $\forall x_i(t)$, $x_j(t) \neq 0$, $i, j \in \{1, 2, \ldots, n\}$, $i \neq j$, we have

$$\frac{\mathrm{d}}{\mathrm{d}t}\left(\frac{x_i(t)}{x_j(t)}\right) = \frac{\dot{x}_i(t) x_j(t) - x_i(t) \dot{x}_j(t)}{x_j^2(t)}. \tag{20}$$

Taking $\dot{x}_i = \kappa(x) x_i$ and $\dot{x}_j = \kappa(x) x_j$ into (20), we can get

$$\frac{\mathrm{d}}{\mathrm{d}t}\left(\frac{x_i(t)}{x_j(t)}\right) = 0. \tag{21}$$

Therefore, we know for $\forall x_i(t)$, $x_j(t) \neq 0$, $i, j \in \{1, 2, \ldots, n\}$, $i \neq j$, $x_i(t)/x_j(t) = c_{ij}$, where $c_{ij} = x_i(0)/x_j(0)$ is a non-zero constant.

Therefore, according to the above discussion, one sufficient condition of TSS is that the system (12) is finite-time stable and the closed-loop state x is ratio persistent. In addition, in the 2- and 3-dimensional space, if the system state is ratio persistent, its trajectory is a straight line, taking the forms $x_1 = c_{12} x_2$, $(x \in \mathbb{R}^2)$ and $x_1 = c_{12} x_2 = c_{12} c_{23} x_3$, $(x \in \mathbb{R}^3)$, respectively. This means that the output generated by a ratio persistent system in $\mathbb{R}^2$ or $\mathbb{R}^3$, is the shortest trajectory between any initial state and the equilibrium.

We are now ready to present the fundamental result of TSS, which will be applied throughout the paper.

Theorem 1: Considering a Lyapunov function $V(x)$, the origin of system (12) is TSS, with the synchronized settling time

$$T(x_0) \leq \frac{V^{1-\alpha}(x_0)}{c(1-\alpha)}, \tag{22}$$

if the following conditions hold:

i. There exist constants $c > 0$ and $\alpha \in (0, 1)$, such that

$$\dot{V}(x) + c V^{\alpha}(x) \leq 0. \tag{23}$$

ii. The state x is ratio persistent.

Proof: Noticing (23) and using Lemma 4, the equilibrium of (12) is clearly finite-time stable with the settling time as in (22).

By contradiction, the rest of the proof is constructed. Assume that at least two state elements x_i and x_j reach the equilibrium at different time instants T_i and T_j. Without loss of generality, let x_j be the last one to arrive, *i.e.*, $T_j > T_i$. According to the property of ratio persistence, we have

$$\lim_{t \to T_i^-} \frac{\mathrm{d}}{\mathrm{d}t}\left(\frac{x_i(t)}{x_j(t)}\right) = 0, \ \lim_{t \to T_i^-} x_i(t) = c_{ij} \lim_{t \to T_i^-} x_j(t), \tag{24}$$

where c_{ij} is a constant value. Since the ratio of each pair of the state elements is kept from the beginning, we have $c_{ij} = x_i(0)/x_j(0)$. Further, since the element x_i arrives at the origin at T_i, it yields

$$\lim_{t \to T_i^-} x_i(t) = 0 \Rightarrow k_{ij} \lim_{t \to T_i^-} x_j(t) = 0. \tag{25}$$

Due to the continuity of the system (12), we have $x_j(T_i) = 0$, where the contradiction occurs because x_j reaches zero at T_j not at T_i. Thus, each pair of the state elements must reach the origin at exactly the same time instant. The proof ends here. ■

Theorem 1 not only provides a sufficient condition to prove TSS but also offers a simple guide to TSC design. This will be detailed in the following sections.

B. Time-Synchronized Control Design

In this subsection, for a comprehensive comparison of TSS and finite-time stability, based on Theorem 1, the NN sign function (5) and the classical sign function (4) are utilized to design a TSC law and a finite-time control law, respectively. Simple first-order affine dynamics in $\mathbb{R}^n$ is considered,

$$\dot{x} = f(x) + b(x) u, \tag{26}$$

where $x = [x_1, x_2, \ldots, x_n]^T \in \mathbb{R}^n$ denotes the state vector, $u \in \mathbb{R}^n$ the control input, and $f(x) \in \mathbb{R}^n$ and $b(x) \in \mathbb{R}^{n\times n}$ ($\det(b(x)) \neq 0$) the known parts.

We now propose a TSC law u_2, and introduce a finite-time control law u_1 for comparison

$$u_1 = -b^{-1}(x)\left(\mathrm{sig}_{\mathrm{c}}^{\alpha}(x) + f(x)\right), \tag{27}$$

$$u_2 = -b^{-1}(x)\left(\mathrm{sig}_{\mathrm{n}}^{\alpha}(x) + f(x)\right), \tag{28}$$

where α is defined as $0 < \alpha = \alpha_1/\alpha_2 < 1$ with positive odd integers α_1 and α_2.

Theorem 2: Under control laws (27) and (28), *i.e.*, $u = u_1$ and $u = u_2$, the system system (26) is finite-time stable and TSS, respectively. In addition, under the controller (28), the closed-loop state x is ratio persistent.

Proof: Consider a Lyapunov function $V_1 = x^T x$. Taking the derivative of V_1, based on the finite-time control law (27), we have $\dot{V}_1 = -2x^T \mathrm{sig}_{\mathrm{c}}^{\alpha}(x) \leq -2V_1^{\frac{\alpha+1}{2}}$. According to Lemma 4, we can derive the settling time of the finite-time convergence $T_1(x_0) \leq V_1^{\frac{1-\alpha}{2}}(x_0)/(1-\alpha)$.

Next, for the system under the TSC law (28), we consider a second Lyapunov function $V_2 = x^T x$. Accordingly, its time derivative reads $\dot{V}_2 = -2x^T \mathrm{sig}_{\mathrm{n}}^{\alpha}(x) = -2V_2^{\frac{\alpha+1}{2}}$. On the other hand, clearly, x is ratio persistent. According to Theorem 1, it proves that the closed-loop system is TSS, and the synchronized settling time is $T_2(x_0) = V_2^{\frac{1-\alpha}{2}}(x_0)/(1-\alpha)$. and the proof ends here. ■

C. Fixed-Time-Synchronized Stability

In this subsection, FTSS is defined, which not only holds the time-synchronized convergence property but is able to additionally obtain an estimation of the synchronized settling time with disregard for the initial state.

Definition 3: (*Fixed-Time-Synchronized Stability*). The equilibrium of the system (12) is *fixed-time-synchronized stable* if

i. it is globally time-synchronized stable in the sense of Definition 1;
ii. the upper bound of the synchronized settling time $T(x_0)$ is independent of any initial system state, i.e., for $\forall x_0$, we have $T(x_0) \leq T_m$, where T_m is a positive constant.

According to Definition 1, FTSS is thus within the scope of fixed-time stability. Next, based on Definition 3, the relevant Lyapunov-type result of FTSS is next addressed.

Theorem 3: Considering a Lyapunov function $V(x)$, the origin of system (12) is FTSS, with the synchronized settling time

$$T(x_0) \leq \frac{1}{\alpha^{\chi}(1-p\chi)} + \frac{1}{\beta^{k}(g\chi-1)}, \tag{29}$$

if the following conditions hold:

i. There exist positive constants α, β, p, g, and χ satisfying $p\chi < 1$ and $g\chi > 1$, such that

$$\dot{V}(x) \leq -(\alpha V^{p}(x) + \beta V^{g}(x))^{\chi}. \tag{30}$$

ii. The state x is ratio persistent.

Proof: Given (30), according to Lemma 5, the system (12) is fixed-time stable with the settling time bounded as in (29). Since x is ratio persistent, the FTSS can be further proved following the contradiction in the proof of Theorem 1. ■

D. Fixed-Time-Synchronized Control Design

In this subsection, to demonstrate FTSS and to consider a class of more practical systems, an FTSC law is designed for second-order systems. Before moving forward, a useful lemma is first proposed.

Lemma 6: Consider the following system dynamics

$$\dot{x} = -\alpha \mathrm{sig}_{\mathrm{n}}^{p}(x) - \beta \mathrm{sig}_{\mathrm{n}}^{g}(x), \tag{31}$$

where $x \in \mathbb{R}^n$ is the state vector, α, β, p and g are positive constants, satisfying $0 < p = p_1^*/p_2^* < 1$ and $1 < g = g_1^*/g_2^*$, with positive odd integers p_1^*, p_2^*, g_1^* and g_2^*. The closed-loop system is ratio persistent and FTSS with the synchronized settling time

$$T_h \leq \frac{2^{\frac{1-p}{2}}}{\alpha(1-p)} + \frac{2^{\frac{1-g}{2}}}{\beta(g-1)}. \tag{32}$$

Proof: Consider a Lyapunov function $V_h = \frac{1}{2}x^T x$. Taking (31) into the derivative of V_h, yields

$$\begin{aligned} \dot{V}_h =& -\alpha x^T \mathrm{sig}_{\mathrm{n}}^{p}(x) - \beta q^T \mathrm{sig}_{\mathrm{n}}^{g}(x) \\ =& -2^{\frac{1+p}{2}} \alpha V_h^{\frac{1+p}{2}} - 2^{\frac{1+g}{2}} \beta V_h^{\frac{1+g}{2}}. \end{aligned} \tag{33}$$

It can be verified that x is ratio persistent. According to Theorem 3, we know that the system (31) is FTSS with the synchronized settling time as shown in (32). ■

As we will present in what follows, the first-order dynamics (31) and its corresponding results given in Lemma 6 actually serve as a basis of the FTSC for more practical system dynamics.

Consider the following second-order affine system

$$\ddot{q} = f(q, \dot{q}) + b(q, \dot{q})\, u, \tag{34}$$

where $q \in \mathbb{R}^n$ and $\dot{q} \in \mathbb{R}^n$, respectively, denote the general position and velocity vectors, $u \in \mathbb{R}^n$ the control input, and $f(q, \dot{q}) \in \mathbb{R}^n$ and $b(q, \dot{q}) \in \mathbb{R}^{n\times n}$ ($\det(b(q, \dot{q})) \neq 0$) are the known parts. The second-order dynamics (34) can be rewritten as an Euler-Lagrange system for applications to mechanical systems, where q stands for the vector of the Lagrangian coordinates.

We design a sliding-mode manifold

$$s = \dot{q} + \alpha_1 \mathrm{sig}_{\mathrm{n}}^{p_1}(q) + \beta_1 \mathrm{sig}_{\mathrm{n}}^{g_1}(q), \tag{35}$$

where α_1 and β_1 are positive constants, and p_1 and g_1 are defined as $0 < p_1 = p_1^*/p_2^* < 1$ and $g_1 = g_1^*/g_2^* > 1$, with positive odd integers p_1^*, p_2^*, g_1^* and g_2^*.

The following FTSC law is then proposed

$$\begin{aligned} u = -b^{-1}(q, \dot{q}) \big(&\alpha_2 \mathrm{sig}_{\mathrm{n}}^{p_2}(s) + \beta_2 \mathrm{sig}_{\mathrm{n}}^{g_2}(s) \\ &+ \rho_1 q q^T \dot{q} + \rho_2 \dot{q} + f(q, \dot{q})\big), \end{aligned} \tag{36}$$

where α_2, β_2, p_2 and g_2 are positive constants, satisfying $0 < p_2 = p_3^*/p_4^* < 1$ and $g_2 = g_3^*/g_4^* > 1$, with positive odd

integers p_3^*, p_4^*, g_3^* and g_4^*, and variables ρ_1 and ρ_2 take the forms

$$\rho_1 = \alpha_1 (p_1 - 1) \|q\|^{p_1 - 3} + \beta_1 (g_1 - 1) \|q\|^{g_1 - 3}, \quad (37)$$

$$\rho_2 = \alpha_1 \|q\|^{p_1 - 1} + \beta_1 \|q\|^{g_1 - 1}. \quad (38)$$

In light of the controller (36), we propose the following theorem.

Theorem 4: Considering the second-order affine system governed by (34), under the FTSC law (36), the closed-loop system is FTSS. The sliding-mode variable s is ratio persistent, while the closed-loop system state q is ratio persistent on the sliding surface $s = 0$.

Proof: Consider a Lyapunov function $V_{h1} = \frac{1}{2} s^T s$. Taking the controller (36) into the derivative of V_{h1}, we have

$$\begin{aligned} \dot{V}_{h1} &= s^T \left(f(q, \dot{q}) + b(q, \dot{q}) u + \rho_1 q q^T \dot{q} + \rho_2 \dot{q} \right) \\ &= -\alpha_2 s^T \mathrm{sig}_{\mathrm{n}}^{p_2}(s) - \beta_2 s^T \mathrm{sig}_{\mathrm{n}}^{g_2}(s) \\ &= -2^{\frac{1+p_2}{2}} \alpha_2 V_{h1}^{\frac{1+p_2}{2}} - 2^{\frac{1+g_2}{2}} \beta_2 V_{h1}^{\frac{1+g_2}{2}}. \end{aligned} \quad (41)$$

Next, taking (36) into the derivative of (35), we can verify that s is ratio persistent. Based on Theorem 3, the sliding mode variable s is FTSS with the synchronized settling time

$$T_{h1} \leq \frac{2^{\frac{1-p_2}{2}}}{\alpha_2 (1 - p_2)} + \frac{2^{\frac{1-g_2}{2}}}{\beta_2 (g_2 - 1)}. \quad (42)$$

Further, on the sliding manifold $s = 0$, we have

$$\dot{q} = -\alpha_1 \mathrm{sig}_{\mathrm{n}}^{p_1}(q) - \beta_1 \mathrm{sig}_{\mathrm{n}}^{g_1}(q). \quad (43)$$

Based on Lemma 6, after the system state arrives at the sliding surface, the closed-loop state q is ratio persistent and FTSS with the synchronized settling time

$$T_{h2} \leq \frac{2^{\frac{1-p_1}{2}}}{\alpha_1 (1 - p_1)} + \frac{2^{\frac{1-g_1}{2}}}{\beta_1 (g_1 - 1)}. \quad (44)$$

The total synchronized settling time of the state q takes the form $T_{hm} \leq T_{h1} + T_{h2}$, which concludes the proof by showing that under the controller (36), the system (34) is FTSS. ■

The FTSC law (36), however, has negative powers -3 and -1 in ρ_1 and ρ_2 (see (37) and (38)), causing a possible singularity problem at the point $q = 0$. To avoid the singularity, we propose a switching sliding mode manifold as

$$s = \dot{q} + s_s. \quad (45)$$

The switching law s_s and its derivative have the forms as in (39) and (40), where ε is a small positive constant, the auxiliary variable s^* takes the form

$$s^* = \dot{q} + \alpha_1 \mathrm{sig}_{\mathrm{n}}^{p_1}(q) + \beta_1 \mathrm{sig}_{\mathrm{n}}^{g_1}(q), \quad (46)$$

constants l_1 and l_2 take the forms

$$l_1 = \alpha_1 \left(\frac{4}{3} - \frac{p_1}{3} \right) \|\varepsilon\|^{p_1 - 1} + \beta_1 \left(\frac{4}{3} - \frac{g_1}{3} \right) \|\varepsilon\|^{g_1 - 1}, \quad (47)$$

$$l_2 = \alpha_1 \left(\frac{p_1}{3} - \frac{1}{3} \right) \|\varepsilon\|^{p_1 - 4} + \beta_1 \left(\frac{g_1}{3} - \frac{1}{3} \right) \|\varepsilon\|^{g_1 - 4}, \quad (48)$$

and the corresponding powers are redefined as

$$\frac{1}{2} < p_1 = p_1^*/p_2^* < 1, \; 1 < g_1 = p_1^*/p_2^* < 4, \quad (49)$$

with positive odd integers p_1^*, p_2^*, g_1^* and g_2^* (the rationality of the value ranges of the parameters p_1 and g_1 will be detailed in Appendixes A and B).

It could be verified that the forms of l_1 and l_2 ensure the continuity of the switching algorithm s_s (39) and $\dot{s}_s$ (40).

Based on the proposed sliding manifold (45), we rewrite the control law (36) as follows,

$$u = -b^{-1}(q, \dot{q}) (\alpha_2 \mathrm{sig}_{\mathrm{n}}^{p_2}(s) + \beta_2 \mathrm{sig}_{\mathrm{n}}^{g_2}(s) + \dot{s}_s + f(q, \dot{q})), \quad (50)$$

where the corresponding powers are defined as $0 < p_2 = p_3^*/p_4^* < 1$ and $g_2 = p_3^*/p_4^* > 1$ with positive odd integers p_3^*, p_4^*, g_3^* and g_4^*.

The main result of this subsection is proposed.

Theorem 5: Considering a second-order system governed by (34), under the singularity-free FTSC law (50), the closed-loop system is FTSS. The sliding-mode variable s is ratio persistent, while the closed-loop system state q is ratio persistent on the sliding surface $s = 0$.

Proof: Consider a Lyapunov function $V_{s1} = \frac{1}{2} s^T s$. Using the control law (50), the derivative of V_{s1} can be written as

$$\dot{V}_{s1} = -2^{\frac{1+p_2}{2}} \alpha_2 V_{s1}^{\frac{1+p_2}{2}} - 2^{\frac{1+g_2}{2}} \beta_2 V_{s1}^{\frac{1+g_2}{2}}. \quad (51)$$

Again, it can be verified that the variable s is ratio persistent. Based on Theorem 3, we know s is FTSS. The corresponding synchronized settling time takes the form

$$T_{s1} \leq \frac{2^{\frac{1-p_2}{2}}}{\alpha_2 (1 - p_2)} + \frac{2^{\frac{1-g_2}{2}}}{\beta_2 (g_2 - 1)}. \quad (52)$$

After the system state q reaches the sliding manifold $s = 0$, we have $\dot{q} = -\alpha_1 \mathrm{sig}_{\mathrm{n}}^{p_1}(q) - \beta_1 \mathrm{sig}_{\mathrm{n}}^{g_1}(q)$, which leads to the ratio persistence of the state q. According to Lemma 6, we know that the closed-loop state is FTSS with the synchronized settling time

$$T_{s2} \leq \frac{2^{\frac{1-p_1}{2}}}{\alpha_1 (1 - p_1)} + \frac{2^{\frac{1-g_1}{2}}}{\beta_1 (g_1 - 1)}, \quad (53)$$

which makes the total setting time of the closed-loop system state q bounded by $T_{sm} \leq T_{s1} + T_{s2}$, and this concludes the proof. ■

Next, the analysis of the singularity problem is given, followed by some further discussion of the stability analysis of the second-order dynamics (34) under the FTSC law (50).

Lemma 7: Using the proposed control law (50) with the switching sliding manifold (45), the singularity problem can be avoided.

Proof: For details, refer to Appendix A. ■

Actually, in light of the switching law (39), $s_s = l_1 q + l_2 \mathrm{sig}_{\mathrm{n}}^4(q)$ only takes place when $s^* \neq 0$, $\|q\| \leq \varepsilon$. We here further discuss the system convergence property before the sliding manifold s converges to the origin ($0 \leq t < T_{s1}$) while $\|q\| \leq \varepsilon$.

Lemma 8: In the case of $s^* \neq 0$, $\|q\| \leq \varepsilon$, under the control law (50) and the switching law (39), the closed-loop system

$$s_s = \begin{cases} \alpha_1 \mathrm{sig}_{\mathrm{n}}^{p_1}(q) + \beta_1 \mathrm{sig}_{\mathrm{n}}^{g_1}(q), & \text{if } s^* = 0 \text{ or } s^* \neq 0,\ \|q\| > \varepsilon, \\ l_1 q + l_2 \mathrm{sig}_{\mathrm{n}}^{4}(q), & \text{if } s^* \neq 0,\ \|q\| \leq \varepsilon, \end{cases} \tag{39}$$

$$\dot{s}_s = \begin{cases} \rho_1 q q^T \dot{q} + \rho_2 \dot{q}, & \text{if } s^* = 0 \text{ or } s^* \neq 0,\ \|q\| > \varepsilon, \\ l_1 \dot{q} + 3 l_2 \|q\| q q^T \dot{q} + l_2 \|q\|^3 \dot{q}, & \text{if } s^* \neq 0,\ \|q\| \leq \varepsilon, \end{cases} \tag{40}$$

(34), viewed as a system with the state q and the input s, is input-to-state stable.

Proof: For details, refer to Appendix B. ∎

Remark 1: By choosing a small enough ε, the state x will converge along the terminal sliding manifold rather than the general sliding manifold to guarantee finite time convergence, *i.e.*, the case of $s^* \neq 0$, $\|x\| \leq \varepsilon$ as in Lemma 8 will not occur during actual convergence. The rationale is similar to the discussion in Remark 4 from [39], which is omitted here.

IV. Illustrative Examples

In this section, we first examine the TSC law as a starting point to show the properties of TSS. Then, to showcase the higher performance of FTSC, a series of simulations are given under different conditions, where interesting properties brought by FTSS are further revealed.

A. Numerical Results of the TSC Law

For the first-order system (26) introduced in Subsection III-B, we here evaluate the performance of the TSC law (28) in comparison with the finite-time controller (27). We consider an extremely simple case for the system (26), where $f(x) = 0$ and $b(x) = I_3$, leading to a single integrator in $\mathbb{R}^3$, $\dot{x} = u$.

Relative simulation examples are given in Figs. 2-3. The simulation parameters are chosen as $x_0 = [1, -3, 6]^T$ and $\alpha = 1/3$. As shown in Figs. 2(a) and 2(b), both control laws (27) and (28) can guarantee that the system state x converges to the origin in finite time. In Fig. 2(a), three state elements converge to the equilibrium separately. It takes x_1 a much longer time to converge as its initial value is far from zero. On the contrary, under the control law (28), TSS is revealed in Fig. 2(b), where x_1, x_2 and x_3 arrive at the origin synchronously.

The 3-dimensional trajectories under the finite-time controller (27) and the TSC law (28) are shown in Fig. 3. It suggests that TSS helps the system generate a smoother and shorter output, as according to Theorem 2 and Definition 2, the trajectory of the closed-loop system under TSC law (28) is ratio persistent, being a (shortest) straight line in the 3-dimensional space.

B. Numerical Results of the FTSC Law

In this subsection, we take the attitude stabilization of a rigid spacecraft as an example, as some highly critical phases of space missions have very strict requirements for the convergence performance of the spacecraft.

First, the spacecraft attitude dynamics are briefly recalled.

1) Spacecraft Attitude Dynamics: We define the cross-product skew symmetric matrix $z^\times$ associated with a vector $z = (z_1, z_2, z_3)^T \in \mathbb{R}^3$ as

$$z^\times = \begin{bmatrix} 0 & -z_3 & z_2 \\ z_3 & 0 & -z_1 \\ -z_2 & z_1 & 0 \end{bmatrix}. \tag{54}$$

Then, utilizing the modified Rodrigues parameters (MRPs) [51], the attitude dynamics with respect to an inertial frame can be represented as

$$\dot{\sigma} = G(\sigma)\,\omega, \tag{55}$$

$$J\dot{\omega} = -\omega^\times J\omega + \tau, \tag{56}$$

where $\sigma \overset{\text{def}}{=} [\sigma_1, \sigma_2, \sigma_3]^T = \tan(\Phi/4)\, e \in \mathbb{R}^3$ denotes the MRPs, $\Phi \in \mathbb{R}$ denotes Euler angle, $e \in \mathbb{R}^3$ the Euler axis, $\omega \overset{\text{def}}{=} [\omega_1, \omega_2, \omega_3]^T \in \mathbb{R}^3$ the angular velocity, $J \in \mathbb{R}^{3\times3}$ the inertia matrix, $\tau \in \mathbb{R}^3$ the control torque, and $G(\sigma) \in \mathbb{R}^{3\times3}$ is given by

$$G(\sigma) = \frac{1}{2}\left(\frac{1 - \sigma^T\sigma}{2} I_3 + \sigma^\times + \sigma\sigma^T\right). \tag{57}$$

Then, (55) and (56) can be rewritten as an Euler-Lagrange equation, that is,

$$M(\sigma)\,\ddot{\sigma} + C(\sigma, \dot{\sigma})\,\dot{\sigma} = u(t), \tag{58}$$

where the relevant parameters are rewritten as

$$M(\sigma) = G^{-T}(\sigma)\, J G^{-1}(\sigma), \tag{59}$$

$$C(\sigma, \dot{\sigma}) = -G^{-T} J G^{-1} \dot{G} G^{-1} - G^{-T} (J\omega)^\times G^{-1}, \tag{60}$$

$$u = G^{-T}(\sigma)\,\tau. \tag{61}$$

Therefore, according to the Euler-Lagrange system (58), we can rewrite the FTSC law (50) for the spacecraft attitude stabilization as

$$u = -M(\sigma)\left(\alpha_2 \mathrm{sig}_{\mathrm{n}}^{p_2}(s) + \beta_2 \mathrm{sig}_{\mathrm{n}}^{g_2}(s) + \dot{s}_s\right) + C(\sigma, \dot{\sigma})\,\dot{\sigma}. \tag{62}$$

2) Fixed-Time Control Law for Comparison: In what follows, to illustrate the features of FTSS, we apply the FTSC law (62) to the spacecraft attitude stabilization. Moreover, to offer a better comparison, we here introduce a fixed-time control (FTC) law for the Euler-Lagrange systems.

Lemma 9: Considering the system governed by (58), under the following FTC law:

$$\bar{u} = -M(\sigma)\left(\alpha_2 \mathrm{sig}_{\mathrm{c}}^{p_2}(\bar{s}) + \beta_2 \mathrm{sig}_{\mathrm{c}}^{g_2}(\bar{s}) + \dot{\bar{s}}_s\right) + C(\sigma, \dot{\sigma})\,\dot{\sigma}. \tag{63}$$

The sliding manifold $\bar{s} = \dot{\sigma} + \bar{s}_s$, the trigger sliding-mode variable $\bar{s}^* = \dot{\sigma} + \alpha_1 \mathrm{sig}_{\mathrm{c}}^{p_1}(\sigma) + \beta_1 \mathrm{sig}_{\mathrm{c}}^{g_1}(\sigma)$, and the switching

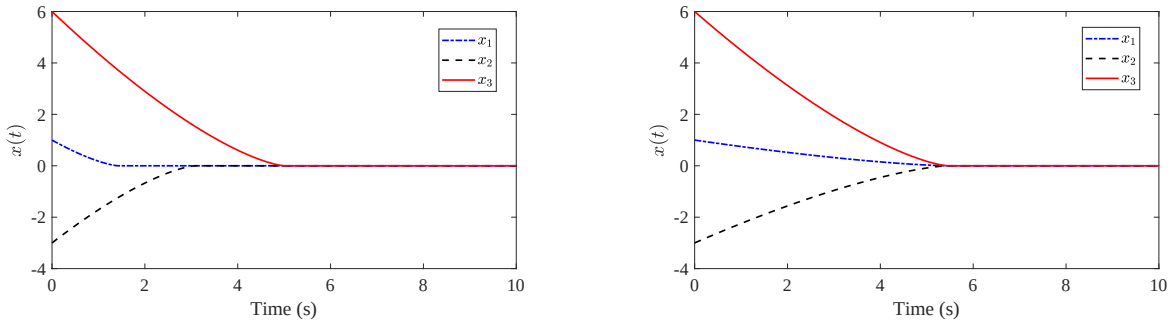

Fig. 2. System state x: (a) performance of the finite-time control law (27); (b) performance of the TSC law (28).

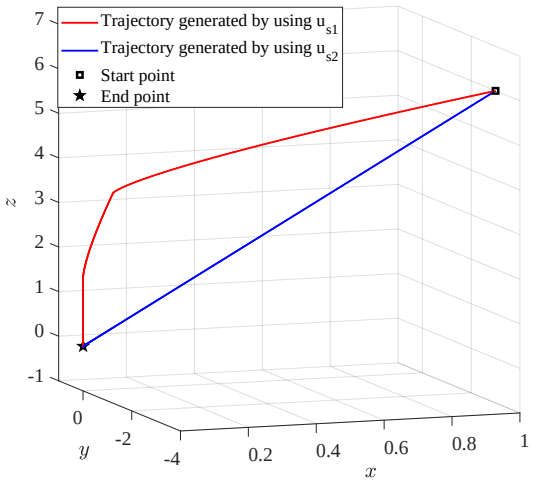

Fig. 3. Comparison of the trajectories under control laws (27) and (28).

law take the forms

$$\bar{s}_{s,i}=\begin{cases}\alpha_1\mathrm{sig}_{\mathrm{c}}^{p_1}(\sigma_i)+\beta_1\mathrm{sig}_{\mathrm{c}}^{g_1}(\sigma_i), & \text{if } \bar{s}^*=0,\\ & \text{or } \bar{s}^*\neq 0, |\sigma_i|>\varepsilon,\\ l_3\sigma_i+l_4\mathrm{sig}_{\mathrm{c}}^{2}(\sigma_i), & \text{if } \bar{s}^*\neq 0, |\sigma_i|\leq\varepsilon,\end{cases}$$

$$\dot{\bar{s}}_{s,i}=\begin{cases}\alpha_1 p_1|\sigma_i|^{p_1-1}\dot{\sigma}_i+\beta_1 g_1|\sigma_i|^{g_1-1}\dot{\sigma}_i, & \text{if } \bar{s}^*=0,\\ & \text{or } \bar{s}^*\neq 0, |\sigma_i|>\varepsilon,\\ l_3\dot{\sigma}+l_4|\sigma_i|\dot{\sigma}_i, & \text{if } \bar{s}^*\neq 0, |\sigma_i|\leq\varepsilon,\end{cases}$$

where σ_i, $\bar{s}_{s,i}$ and $\dot{\bar{s}}_{s,i}$ denote the ith element of σ, $\bar{s}_s$ and $\dot{\bar{s}}_s$, $i=1,2,...,n$. l_3 and l_4 take the following forms to guarantee the continuity of $\bar{s}_s$ and $\dot{\bar{s}}_s$:

$$l_3=(2-p_1)\alpha_1\varepsilon^{p_1-1}+(2-g_1)\beta_1\varepsilon^{g_1-1}, \tag{64}$$

$$l_4=(p_1-1)\alpha_1\varepsilon^{p_1-2}+(g_1-1)\beta_1\varepsilon^{g_1-2}. \tag{65}$$

The closed-loop system state converges to the origin in fixed time.

Proof: The proof is omitted due to page limit, which can be given following the procedure in [39]. ■

3) Control Performance of FTSC and FTC: In Table II, the simulation parameters for the FTSC law (62) and the FTC law (63) are provided, where the control parameters for both the controllers are identical for fairness of comparison.

Using the FTC law (63) and the FTSC law (62), the corresponding closed-loop system states are respectively shown

TABLE II
SIMULATION PARAMETERS: CASE 1

Parameters	Values	Parameters	Values
α_1	0.1	p_1	0.65
α_2	0.05	p_2	0.65
β_1	0.1	g_1	1.1
β_2	0.05	g_2	1.1
σ_0	$[0.06,-0.03,0.01]^T$	ε	0.0001
J	$[12,0.4,0.2;0.4,10,0.6;0.2,0.6,11]$		$(\mathrm{kg}\cdot\mathrm{m}^2)$

in Figs. 4(a) and 4(b). In Fig. 4(a), it explicitly indicates that under the FTC law (63), three state elements σ_1, σ_2 and σ_3 converge to the origin separately at different time instants, while as shown in Fig. 4(b), the FTSC law (62) synchronously drives all the state elements to the equilibrium. For greater clarity, the norms of the state elements governed by two control laws are given in Figs. 5(a) and 5(b). In Fig. 5(a), the state element σ_3 arrive at the origin first at $t=16s$, and then the other two elements catch up at $t=22s$ and $t=26s$. On the contrary, all the state elements in Fig. 5(b), reach the origin synchronously at $t=26s$.

Moreover, in Fig. 6, it demonstrates that the state trajectory generated by the FTSC law (62) is ratio persistent, making the whole trajectory shorter compared with that governed by the FTC law (63), as it is a straight line between the start point and the end point.

Specifically, the property of ratio persistence is further shown in Fig. 7(a), where we have

$$\frac{\sigma_1(t)}{\sigma_2(t)}=\frac{\sigma_1(0)}{\sigma_2(0)}=-2, \tag{66}$$

$$\frac{\sigma_1(t)}{\sigma_3(t)}=\frac{\sigma_1(0)}{\sigma_3(0)}=6, \tag{67}$$

$$\frac{\sigma_2(t)}{\sigma_3(t)}=\frac{\sigma_2(0)}{\sigma_3(0)}=-3. \tag{68}$$

It also evidently approves declared FTSS under the FTSC law (62). Finally, the relevant control inputs of the FTSC law (62) are given in Fig. 7(b). One may wonders why the ratios in Fig. 7(a) do not run into a singularity $0/0$ after the state elements converge to the origin. It is because the simulation software has a limit on the numerical resolution (*e.g.*, by default, MATLAB® uses 16 digits of precision).

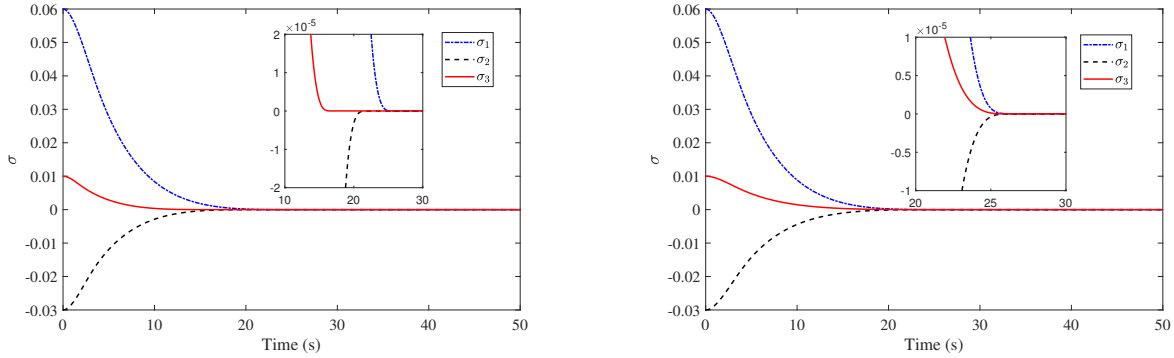

(a) (b)

Fig. 4. System state σ: (a) performance of the FTC law (63); (b) performance of the FTSC law (62).

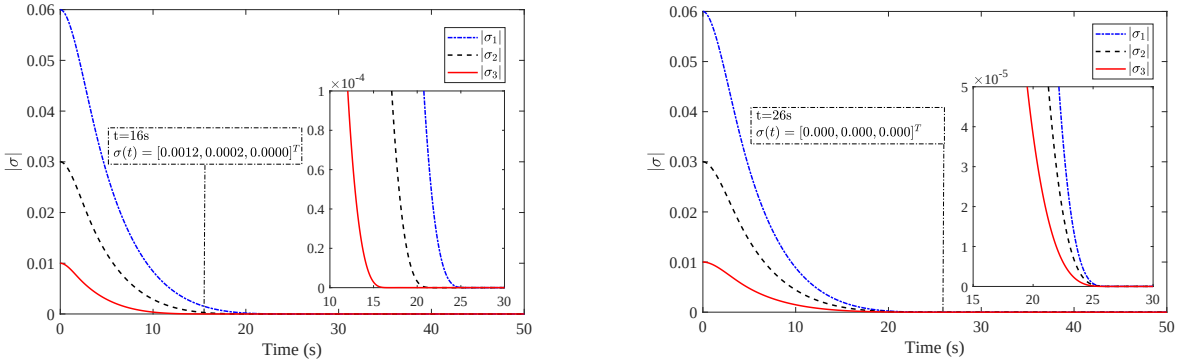

(a) (b)

Fig. 5. Norm of the system state σ: (a) performance of the FTC law (63); (b) performance of the FTSC law (62).

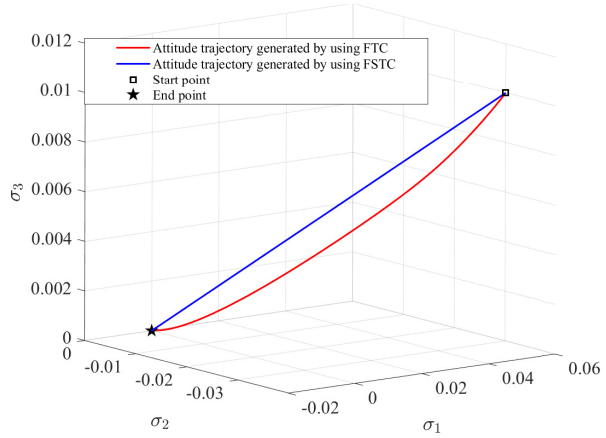

Fig. 6. Comparison of the attitude trajectories under the FTC law (63) and the FTSC law (62). (Please note that these trajectories are not the real movements of the spacecraft attitude, as modified Rodrigues parameters are applied in the system dynamics.)

Thus, although σ_i and σ_j can reach the origin theoretically, they might be respectively represented as $\sigma_i = 6 * 10^{-15}$ and $\sigma_j = 1 * 10^{-15}$ in the simulation software, making their ratio remains to be a constant with the value of 6.

Next, for a more comprehensive comparison, we choose another set of parameters for simulation as shown in Table III. Basically, the power parameters p_1, p_2, g_1 and g_2 are re-selected (as they are the crucial ones to affect the performance), while the other parameters remain the same.

TABLE III
SIMULATION PARAMETERS: CASE 2

Parameters	Values	Parameters	Values
α_1	0.1	p_1	0.7
α_2	0.05	p_2	0.7
β_1	0.1	g_1	1.2
β_2	0.05	g_2	1.2
σ_0	$[0.06, -0.03, 0.01]^T$	ε	0.0001
J	$[12, 0.4, 0.2; 0.4, 10, 0.6; 0.2, 0.6, 11]$		(kg·m^2)

Here, we directly plot the norms of the state elements under two controllers in Figs. 8(a) and 8(b). Again, Fig. 8(a) shows that the time-synchronized convergence property cannot be expected from the FTC law (63). The main reason is that the classical sign function sig_c decouples a vector into different scalar while the NN sign function sig_n incorporates the normalization of a vector with its specified norm. Due to the same reason, in Fig. 8(b), FTSS is successfully achieved at $t = 20s$. It is additionally noticeable that there exist overshoots in Fig. 8(a), which inevitably degrades the system performance, while no such deterioration can be found in Fig. 8(b).

Compared with the simulation results in the first case (see Figs. 5(a) and 5(b)), the difference between the control

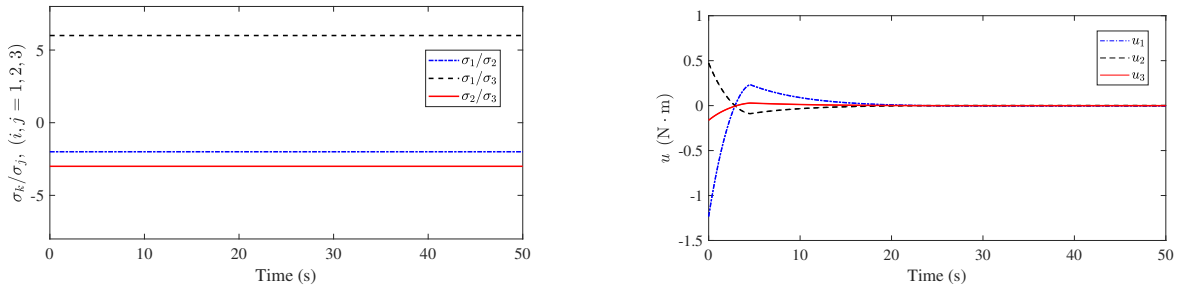

(a) (b)

Fig. 7. Performance of the FTSC law (62): (a) ratio of the elements of the system state σ; (b) control inputs.

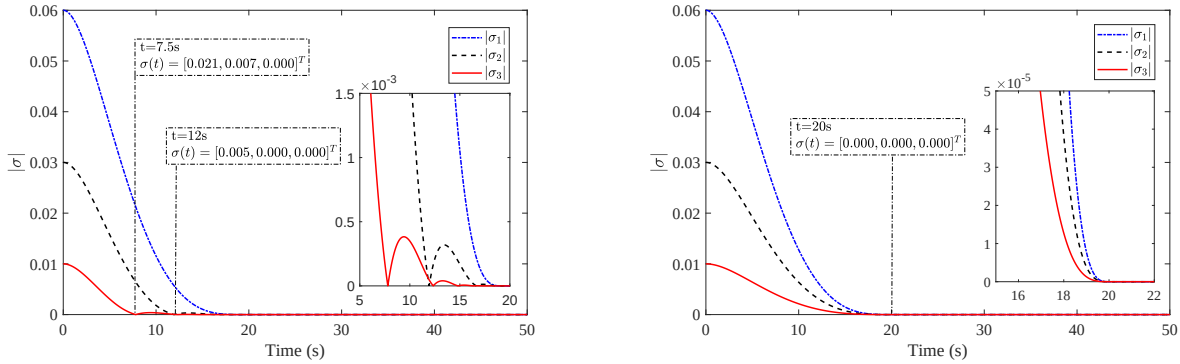

(a) (b)

Fig. 8. Norm of the system state σ: (a) performance of the FTC law (63); (b) performance of the FTSC law (62).

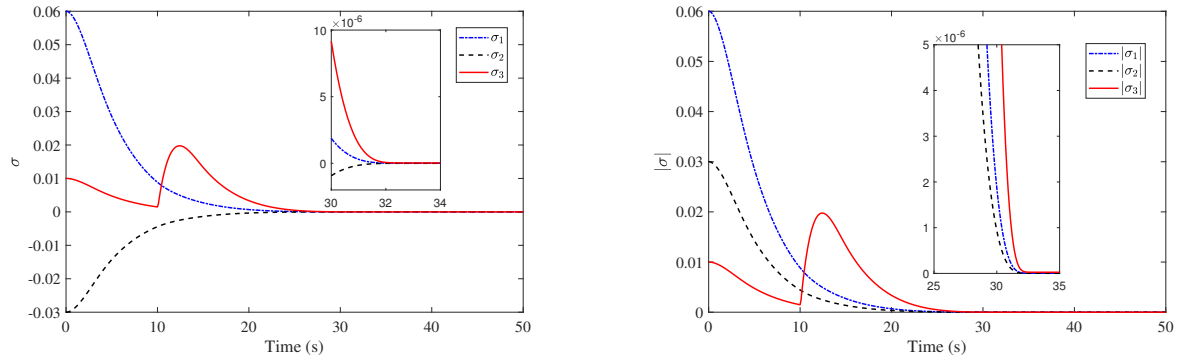

(a) (b)

Fig. 9. Performance of the FTSC law (62) with an impulsive disturbance: (a) System state σ; (b) Norm of the system state σ.

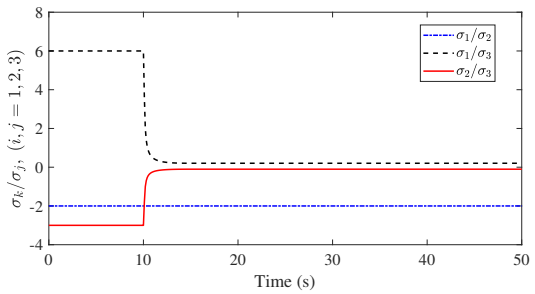

Fig. 10. Ratio of the state elements using FTSC (62) under an impulsive disturbance.

performances of the two controllers become more obvious in Figs. 8(a) and 8(b). For example, the trajectories of the state elements in Figs. 5(a) and 5(b) are similar to a certain degree (although their times of arrival to the origin are different), while in Figs. 8(a) and 8(b), the differences of trajectories are more distinct. It is conjectured empirically from numerous simulations that a decrease in p_1 and p_2 or an increase in g_1 and g_2 leads to a greater difference between the performances of the FTSC law (62) and the FTC law (63).

So far, we have presented two simulation cases to reveal the nature of FTSS. Moreover, compared with the FTC law (63), the property of ratio persistence has been clearly illustrated. Note that all the current results assume that there exists

no external disturbance. In real-world applications, however, disturbances are inevitable and sometimes unpredictable.

Therefore, to further evaluate the FTSC law (62) under disturbances, additional simulations are conducted, where all the control parameters are chosen the same as shown in Table II. We here consider that the system suffers from an external impulsive disturbance that acts on the state element σ_3 at $t = 10s$. The relevant numerical results are presented in Figs. 9-10. It is shown in Figs. 9(a) and 9(b) that despite the external disturbance, FTSS is still achieved successfully. The rationale lies in that although σ_3 drifts significantly because of the disturbance, the FTSC law (62) continues generating a proper control input, intending to preserve the ratio persistent property of the current system state. Thus in Fig. 10, after the impulsive disturbance, the ratio of each affected pair of the state elements quickly converged to a new constant.

V. Conclusion

This paper has shown unique and deeper insight into the established finite-time stability, by defining a (fixed-) time-synchronized control problem with (fixed-) time-synchronized stability, and formulating Lyapunov stability results. The notion of ratio persistence has been defined to facilitate the achievement of such a (fixed-) time-synchronized convergence property. A series of control laws have been proposed for first-order and for second-order systems to achieve (fixed-) time-synchronized stability. Furthermore, the singularity-free control has been designed for second-order systems. A notable challenge lies in that some state of the art techniques subjected to the classical sign function, cannot be directly applied to such (fixed-) time-synchronized control design.

It is found here that, while both of the classical sign function and the norm-normalized sign function help to stabilize a system, the norm-normalized sign function additionally empowers the system to achieve (fixed-) time-synchronized stability. It is noteworthy that this norm-normalized sign function is of theoretical importance and has wide applicability not only in control system design but also in fields of engineering and various other sciences, which possibly endows this approach an extended contribution. Nevertheless, clearly various important directions remain open, *e.g.*, while we have elaborated on how to extend this approach from first-order systems to second-order systems, there are certainly indeed yet more complex systems with difficult practical issues which should be considered in future work.

Acknowledgment

The authors would like to extend their gratitude towards the support and fruitful discussions of Dr. J. Qian from Stony Brook University, New York, Dr. K. Cao from Nanyang Technological University, Dr. Z. Hou from National University of Singapore, and Dr. H. Jiang from Harbin Institute of Technology.

Appendix A
Proof of Lemma 7

The proof can be given by the following three cases.

Case 1: $\|q\| > \varepsilon$. It is trivial that there is no singularity problem.

Case 2: $\|q\| \leq \varepsilon$, $s^* = 0$. According to the switching law (39), we have

$$\dot{q} = -\alpha_1 \mathrm{sig}_{\mathrm{n}}^{p_1}(q) - \beta_1 \mathrm{sig}_{\mathrm{n}}^{g_1}(q). \tag{69}$$

Substituting (69) into the control law (50) yields,

$$\begin{aligned} u = &- b^{-1}(q,\dot{q})\left(\alpha_2 \mathrm{sig}_{\mathrm{n}}^{p_2}(s) + \beta_2 \mathrm{sig}_{\mathrm{n}}^{g_2}(s)\right. \\ &\left. + Q + f(q,\dot{q})\right), \end{aligned} \tag{70}$$

where we define

$$\begin{aligned} Q = &\rho_1 q q^T \alpha_1 \mathrm{sig}_{\mathrm{n}}^{p_1}(q) + \rho_1 q q^T \beta_1 \mathrm{sig}_{\mathrm{n}}^{g_1}(q) \\ &+ \rho_2 \alpha_1 \mathrm{sig}_{\mathrm{n}}^{p_1}(q) + \rho_2 \beta_1 \mathrm{sig}_{\mathrm{n}}^{g_1}(q). \end{aligned} \tag{71}$$

Substituting ρ_1 and ρ_2 (see (37)-(38)) into (71), we have

$$\begin{aligned} Q = &\alpha_1(p_1-1)\|q\|^{p_1-3} q q^T \alpha_1 \mathrm{sig}_{\mathrm{n}}^{p_1}(q) \\ &+ \beta_1(g_1-1)\|q\|^{g_1-3} q q^T \alpha_1 \mathrm{sig}_{\mathrm{n}}^{p_1}(q) \\ &+ \alpha_1(p_1-1)\|q\|^{p_1-3} q q^T \beta_1 \mathrm{sig}_{\mathrm{n}}^{g_1}(q) \\ &+ \beta_1(g_1-1)\|q\|^{g_1-3} q q^T \beta_1 \mathrm{sig}_{\mathrm{n}}^{g_1}(q) \\ &+ \left(\alpha_1\|q\|^{p_1-1} + \beta_1\|q\|^{g_1-1}\right)\alpha_1 \mathrm{sig}_{\mathrm{n}}^{p_1}(q) \\ &+ \left(\alpha_1\|q\|^{p_1-1} + \beta_1\|q\|^{g_1-1}\right)\beta_1 \mathrm{sig}_{\mathrm{n}}^{g_1}(q). \end{aligned} \tag{72}$$

Based on Lemma 3, we know

$$q q^T \mathrm{sig}_{\mathrm{n}}^{p_1}(q) = \mathrm{sig}_{\mathrm{n}}^{p_1+2}(q). \tag{73}$$

Taking (73) into (72), it reads

$$\begin{aligned} Q = &\alpha_1^2(p_1-1)\mathrm{sig}_{\mathrm{n}}^{2p_1-1}(q) + \alpha_1\beta_1(g_1-1)\mathrm{sig}_{\mathrm{n}}^{p_1+g_1-1}(q) \\ &+ \alpha_1\beta_1(p_1-1)\mathrm{sig}_{\mathrm{n}}^{p_1+g_1-1}(q) + \beta_1^2(g_1-1)\mathrm{sig}_{\mathrm{n}}^{2g_1-1}(q) \\ &+ \alpha_1^2 \mathrm{sig}_{\mathrm{n}}^{2p_1-1}(q) + \alpha_1\beta_1 \mathrm{sig}_{\mathrm{n}}^{p_1+g_1-1}(q) \\ &+ \alpha_1\beta_1 \mathrm{sig}_{\mathrm{n}}^{p_1+g_1-1}(q) + \beta_1^2 \mathrm{sig}_{\mathrm{n}}^{2g_1-1}(q) \\ = &\alpha_1^2 p_1 \mathrm{sig}_{\mathrm{n}}^{2p_1-1}(q) + \beta_1^2 g_1 \mathrm{sig}_{\mathrm{n}}^{2g_1-1}(q) \\ &+ \alpha_1\beta_1(p_1+g_1)\mathrm{sig}_{\mathrm{n}}^{p_1+g_1-1}(q). \end{aligned} \tag{74}$$

Since we know $\frac{1}{2} < p_1 < 1$ and $g_1 > 1$, the singularity can thus be avoided in (74) as $2p_1 - 1 > 0$, $2g_1 - 1 > 0$, and $p_1 + g_1 - 1 > 0$.

Case 3: $\|q\| \leq \varepsilon$, $s^* \neq 0$, the sliding manifold (45) becomes a general one without any singularity by the switching law (39). Therefore, according to the above discussion, the singularity problem can be avoided. This finishes the proof. ■

Appendix B
Proof of Lemma 8

Before moving on, relevant necessary results on input-to-state stability are first recalled.

Definition 4: [52] Consider a general nonlinear system

$$\dot{x} = f(x,u),\ f(0,0) = 0,\ x(0) = x_0, \tag{75}$$

where $f : \mathbb{R}^n \times \mathbb{R}^m \to \mathbb{R}^n$ is continuously differentiable. The system (75) is input-to-state stable (ISS) if there exist a

$\mathcal{KL}$-function γ_1 and a $\mathcal{K}$-function γ_2 such that, for each input $u \in L_\infty$ and each $x_0 \in \mathbb{R}^n$, it holds that

$$|x(t, x_0, u)| \leq \gamma_1(|x_0|, t) + \gamma_2(\|u\|), \ \forall t \geq 0. \tag{76}$$

Definition 5: [52] A smooth function $V : \mathbb{R}^n \to \mathbb{R}_+$ is an ISS Lyapunov function if there exist functions $\alpha_1, \alpha_2 \in \mathcal{K}_\infty$ and $\alpha_3, \ell \in \mathcal{K}$, such that for $\forall x \in \mathbb{R}^n, u \in \mathbb{R}^m$, the following conditions hold

$$\alpha_1(|x|) \leqslant V(x) \leqslant \alpha_2(|x|), \tag{77}$$
$$|x| \geqslant \ell(|u|) \Rightarrow L_{f(x,u)}V(x) \leqslant -\alpha_3(|x|), \tag{78}$$

where ℓ is the Lyapunov gain.

Lemma 10: [52] The system (75) is ISS iff it there exists an ISS Lyapunov function for it.

The proof of Lemma 8 can then be addressed as follows.

In the case of $s^* \neq 0$, $\|q\| \leq \varepsilon$, according to the switching law (39), we have

$$\dot{q} = -l_1 q - l_2 \mathrm{sig}_{\mathrm{n}}^4(q) + s. \tag{79}$$

Consider a Lyapunov function

$$V_{ISS} = \frac{1}{2} q^T q. \tag{80}$$

Its time derivative takes the form

$$\begin{aligned} \dot{V}_{ISS} =& -l_1 q^T q - l_2 \|q\|^3 q^T q + q^T s \\ =& -\left(l_1 + l_2 \|q\|^3\right) q^T q + q^T s. \end{aligned} \tag{81}$$

Denoting $L = l_1 + l_2\|q\|^3$, based on (47) and (48), we have

$$\begin{aligned} L =& \alpha_1 \left(\frac{4}{3} - \frac{p_1}{3}\right) \|\varepsilon\|^{p_1 - 1} + \alpha_1 \left(\frac{p_1}{3} - \frac{1}{3}\right) \|\varepsilon\|^{p_1 - 4} \|q\|^3 \\ &+ \beta_1 \left(\frac{4}{3} - \frac{g_1}{3}\right) \|\varepsilon\|^{g_1 - 1} + \beta_1 \left(\frac{g_1}{3} - \frac{1}{3}\right) \|\varepsilon\|^{g_1 - 4} \|q\|^3. \end{aligned}$$

Noticing $1 < g_1 < 4$ and $\|q\| \leq \varepsilon$, we thus can get

$$\begin{aligned} L \geq& \alpha_1 \left(\frac{4}{3} - \frac{p_1}{3}\right) \|\varepsilon\|^{p_1 - 1} + \alpha_1 \left(\frac{p_1}{3} - \frac{1}{3}\right) \|\varepsilon\|^{p_1 - 1} \\ &+ \beta_1 \left(\frac{4}{3} - \frac{g_1}{3}\right) \|\varepsilon\|^{g_1 - 1}. \end{aligned} \tag{82}$$

Define a positive constant

$$\lambda = \alpha_1 \|\varepsilon\|^{p_1 - 1} + \beta_1 \left(\frac{4}{3} - \frac{g_1}{3}\right) \|\varepsilon\|^{g_1 - 1}. \tag{83}$$

Therefore, (81) becomes

$$\begin{aligned} \dot{V}_{ISS} \leq& -\lambda q^T q + q^T s \\ =& -\lambda (1 - \theta) q^T q - \left(\lambda \theta q^T q - q^T s\right), \end{aligned} \tag{84}$$

where $\theta \in (0, 1)$.

Then, for $\lambda \theta q^T q - q^T s > 0$, we have

$$\dot{V}_{ISS} \leq -\lambda (1 - \theta) q^T q. \tag{85}$$

By taking

$$\kappa_1(\delta) = \lambda (1 - \theta) \|\delta\|^2 \tag{86}$$
$$\kappa_2(\delta) = \frac{\|\delta\|}{\lambda \theta}, \tag{87}$$

where the variable $\delta \in \mathbb{R}^n$, we obtain that

$$\dot{V}_{ISS} \leq -\kappa_1(q), \tag{88}$$

if $\|q\| \geq \kappa_2(s)$. This concludes the proof by showing that, according to Definition 5 and Lemma 10, the closed-loop system is ISS. The corresponding ISS-Lyapunov function is $V_{ISS}(q) = \frac{1}{2} q^T q$, with the Lyapunov gain $\kappa_2(s)$.

REFERENCES

[1] H. Du, S. Li, and C. Qian, "Finite-time attitude tracking control of spacecraft with application to attitude synchronization," *IEEE Transactions on Automatic Control*, vol. 56, no. 11, pp. 2711–2717, 2011.

[2] B. Xiao, Q. Hu, and Y. Zhang, "Adaptive sliding mode fault tolerant attitude tracking control for flexible spacecraft under actuator saturation," *IEEE Transactions on Control Systems Technology*, vol. 20, no. 6, pp. 1605–1612, 2011.

[3] A.-M. Zou, K. D. Kumar, Z.-G. Hou, and X. Liu, "Finite-time attitude tracking control for spacecraft using terminal sliding mode and Chebyshev neural network," *IEEE Transactions on Systems, Man, and Cybernetics, Part B (Cybernetics)*, vol. 41, no. 4, pp. 950–963, 2011.

[4] M. Galicki, "Finite-time control of robotic manipulators," *Automatica*, vol. 51, pp. 49–54, 2015.

[5] C. Yang, Y. Jiang, J. Na, Z. Li, L. Cheng, and C.-Y. Su, "Finite-time convergence adaptive fuzzy control for dual-arm robot with unknown kinematics and dynamics," *IEEE Transactions on Fuzzy Systems*, vol. 27, no. 3, pp. 574–588, 2018.

[6] D. Zhai and Y. Xia, "Finite-Time Control of Teleoperation Systems With Input Saturation and Varying Time Delays," *IEEE Transactions on Systems, Man, and Cybernetics: Systems*, vol. 47, no. 7, pp. 1522–1534, 2017.

[7] G. Li, X. Wang, and S. Li, "Finite-Time Output Consensus of Higher-Order Multiagent Systems With Mismatched Disturbances and Unknown State Elements," *IEEE Transactions on Systems, Man, and Cybernetics: Systems*, vol. 49, no. 12, pp. 2571–2581, 2019.

[8] S. Khoo, L. Xie, and Z. Man, "Robust finite-time consensus tracking algorithm for multirobot systems," *IEEE/ASME Transactions on Mechatronics*, vol. 14, no. 2, pp. 219–228, 2009.

[9] M. Van, M. Mavrovouniotis, and S. S. Ge, "An Adaptive Backstepping Nonsingular Fast Terminal Sliding Mode Control for Robust Fault Tolerant Control of Robot Manipulators," *IEEE Transactions on Systems, Man, and Cybernetics: Systems*, vol. 49, no. 7, pp. 1448–1458, 2019.

[10] D. Li, S. S. Ge, W. He, G. Ma, and L. Xie, "Multilayer formation control of multi-agent systems," *Automatica*, vol. 109, p. 108558, 2019.

[11] R. Engel and G. Kreisselmeier, "A continuous-time observer which converges in finite time," *IEEE Transactions on Automatic Control*, vol. 47, no. 7, pp. 1202–1204, 2002.

[12] F. J. Bejarano and L. Fridman, "High order sliding mode observer for linear systems with unbounded unknown inputs," *International Journal of Control*, vol. 83, no. 9, pp. 1920–1929, 2010.

[13] W. Perruquetti, T. Floquet, and E. Moulay, "Finite-time observers: application to secure communication," *IEEE Transactions on Automatic Control*, vol. 53, no. 1, pp. 356–360, 2008.

[14] V. T. Haimo, "Finite time controllers," *SIAM Journal on Control and Optimization*, vol. 24, no. 4, pp. 760–770, 1986.

[15] A. Polyakov, "Nonlinear feedback design for fixed-time stabilization of linear control systems," *IEEE Transactions on Automatic Control*, vol. 57, no. 8, pp. 2106–2110, 2012.

[16] I.-S. Jeon, J.-I. Lee, and M.-J. Tahk, "Homing guidance law for cooperative attack of multiple missiles," *Journal of guidance, control, and dynamics*, vol. 33, no. 1, pp. 275–280, 2010.

[17] D. Li, S. S. Ge, and T. H. Lee, "Simultaneous-Arrival-to-Origin Convergence," *Under Review*, 2020.

[18] H. K. Khalil, *Nonlinear systems*. New Jersey: Prentice hall, 1996.

[19] J. D. Roberts, "Linear model reduction and solution of the algebraic Riccati equation by use of the sign function," *International Journal of Control*, vol. 32, no. 4, pp. 677–687, 1980.

[20] C. S. Kenney and A. J. Laub, "The matrix sign function," *IEEE Transactions on Automatic Control*, vol. 40, no. 8, pp. 1330–1348, 1995.

[21] V. I. Utkin, "Sliding mode control design principles and applications to electric drives," *IEEE transactions on industrial electronics*, vol. 40, no. 1, pp. 23–36, 1993.

[22] Y. Cao, Y. Song, and C. Wen, "Practical tracking control of perturbed uncertain nonaffine systems with full state constraints," *Automatica*, vol. 110, p. 108608, 2019.

[23] Y. Cao, W. Ren, and Z. Meng, "Decentralized finite-time sliding mode estimators and their applications in decentralized finite-time formation tracking," *Systems & Control Letters*, vol. 59, no. 9, pp. 522–529, 2010.

[24] A. Zavala-Rio and I. Fantoni, "Global finite-time stability characterized through a local notion of homogeneity," *IEEE Transactions on Automatic Control*, vol. 59, no. 2, pp. 471–477, 2014.

[25] M. Van, S. S. Ge, and H. Ren, "Robust Fault-Tolerant Control for a Class of Second-Order Nonlinear Systems Using an Adaptive Third-Order Sliding Mode Control," *IEEE Transactions on Systems, Man, and Cybernetics: Systems*, vol. 47, no. 2, pp. 221–228, 2017.

[26] G. Rinaldi, P. P. Menon, C. Edwards, and A. Ferrara, "Higher Order Sliding Mode Observers in Power Grids With Traditional and Renewable Sources," *IEEE Control Systems Letters*, vol. 4, no. 1, pp. 223–228, 2019.

[27] C. Yang, D. Huang, W. He, and L. Cheng, "Neural Control of Robot Manipulators With Trajectory Tracking Constraints and Input Saturation," *IEEE Transactions on Neural Networks and Learning Systems in press, DOI: 10.1109/TNNLS.2020.3017202*, 2020.

[28] K. D. Young, V. I. Utkin, and Ü. Özgüner, "A control engineer's guide to sliding mode control," *IEEE Transactions on Control Systems Technology*, vol. 7, no. 3, pp. 328–342, 1999.

[29] X. Yu and O. Kaynak, "Sliding-mode control with soft computing: A survey," *IEEE Transactions on Industrial Electronics*, vol. 56, no. 9, pp. 3275–3285, 2009.

[30] H. Ma, H. Li, R. Lu, and T. Huang, "Adaptive event-triggered control for a class of nonlinear systems with periodic disturbances," *Science China Information Sciences*, vol. 63, pp. 1–15, 2020.

[31] C. Edwards and S. Spurgeon, *Sliding mode control: Theory and applications*. Crc Press, 1998.

[32] S. S. Ge, T. H. Lee, and C. J. Harris, *Adaptive neural network control of robotic manipulators*. London, UK: World Scientific, 1998.

[33] V. Utkin, J. Guldner, and J. Shi, *Sliding Mode Control in Electro-Mechanical Systems*. CRC Press, 2009.

[34] M. T. Hamayun, C. Edwards, and H. Alwi, "Design and analysis of an integral sliding mode fault-tolerant control scheme," *IEEE Transactions on Automatic Control*, vol. 57, no. 7, pp. 1783–1789, 2012.

[35] A. K. Sanyal and J. Bohn, "Finite-time stabilisation of simple mechanical systems using continuous feedback," *International Journal of Control*, vol. 88, no. 4, pp. 783–791, 2015.

[36] D. Li, S. S. Ge, and T. H. Lee, "Fixed-Time-Synchronized Consensus Control of Multi-Agent Systems," *IEEE Transactions on Control of Network Systems, in press, DOI: 10.1109/TCNS.2020.3034523*, 2020.

[37] Z. Zuo, "Nonsingular fixed-time consensus tracking for second-order multi-agent networks," *Automatica*, vol. 54, pp. 305–309, 2015.

[38] ——, "Non-singular fixed-time terminal sliding mode control of non-linear systems," *IET control theory & applications*, vol. 9, no. 4, pp. 545–552, 2014.

[39] L. Wang, T. Chai, and L. Zhai, "Neural-network-based terminal sliding-mode control of robotic manipulators including actuator dynamics," *IEEE Transactions on Industrial Electronics*, vol. 56, no. 9, pp. 3296–3304, 2009.

[40] K. Lu and Y. Xia, "Adaptive attitude tracking control for rigid spacecraft with finite-time convergence," *Automatica*, vol. 49, no. 12, pp. 3591–3599, 2013.

[41] B. Jiang, Z. Chen, Q. Hu, and J. Qi, "Fixed-time attitude control for rigid spacecraft with actuator saturation and faults," *IEEE Transactions on Control Systems Technology*, vol. 24, no. 5, pp. 4375–4380, 2014.

[42] Y. Feng, X. Yu, and Z. Man, "Non-singular terminal sliding mode control of rigid manipulators," *Automatica*, vol. 38, no. 12, pp. 2159–2167, 2002.

[43] L. Yang and J. Yang, "Nonsingular fast terminal sliding-mode control for nonlinear dynamical systems," *International Journal of Robust and Nonlinear Control*, vol. 21, no. 16, pp. 1865–1879, 2011.

[44] J. Yang, S. Li, J. Su, and X. Yu, "Continuous nonsingular terminal sliding mode control for systems with mismatched disturbances," *Automatica*, vol. 49, no. 7, pp. 2287–2291, 2013.

[45] Y. Feng, X. Yu, and F. Han, "On nonsingular terminal sliding-mode control of nonlinear systems," *Automatica*, vol. 49, no. 6, pp. 1715–1722, 2013.

[46] S. P. Bhat and D. S. Bernstein, "Finite-time stability of continuous autonomous systems," *SIAM Journal on Control and Optimization*, vol. 38, no. 3, pp. 751–766, 2000.

[47] B. Zhou, "Finite-time stability analysis and stabilization by bounded linear time-varying feedback," *Automatica*, vol. 121, p. 109191, 2020.

[48] V. I. Utkin, *Sliding Modes in Control and Optimization*. Springer Berlin Heidelberg, 1992.

[49] S. Gutman, "Uncertain dynamical systems–A Lyapunov min-max approach," *IEEE Transactions on Automatic Control*, vol. 24, no. 3, pp. 437–443, 1979.

[50] A. Levant and B. Shustin, "Quasi-Continuous MIMO Sliding-Mode Control," *IEEE Transactions on Automatic Control*, vol. 63, no. 9, pp. 3068–3074, 2018.

[51] J. Ahmed, V. T. Coppola, and D. S. Bernstein, "Adaptive asymptotic tracking of spacecraft attitude motion with inertia matrix identification," *Journal of Guidance, Control, and Dynamics*, vol. 21, no. 5, pp. 684–691, 1998.

[52] E. D. Sontag and Y. Wang, "On characterizations of the input-to-state stability property," *Systems & Control Letters*, vol. 24, no. 5, pp. 351–359, 1995.

Dongyu Li (S'16-M'19) received the B.S. and Ph.D. degree from Control Science and Engineering, Harbin Institute of Technology, China, in 2016 and 2020. He was a joint Ph.D. student supported with the Department of Electrical and Computer Engineering at National University of Singapore, where he is currently a research fellow with the Department of Biomedical Engineering. His research interests include networked system cooperation, robotic control, and human-robot interaction.

Haoyong Yu (SM'19) received the B.S. and M.S. degrees in Mechanical Engineering from Shanghai Jiao Tong University, Shanghai, China, in 1988 and 1991 respectively. He received the Ph.D. degree in Mechanical Engineering from Massachusetts Institute of Technology, Cambridge, Massachusetts, USA, in 2002. He is currently an Associate Professor with the Department of Biomedical Engineering at National University of Singapore. His areas of research include medical robotics, rehabilitation engineering and assistive technologies, system dynamics and control.

Keng Peng Tee (S'04–M'08) received the B.Eng. (first class honors), M.Eng., and Ph.D. degrees in 2001, 2003, and 2008, respectively, all from the National University of Singapore, Singapore. Keng Peng Tee is currently a Senior Scientist at A*STAR's Institute for Infocomm Research, where he holds an appointment as Head of Manipulation Unit in the Robotics Department. His active research interests include manipulation learning, adaptive systems, and human–robot collaboration.

Yan Wu (M'08-SM'17) received the B.A. degree in engineering from the University of Cambridge, U.K., in 2007, and the Ph.D. degree in electrical engineering from Imperial College London, U.K., in 2013. From 2012 to 2013, he joined both the Institute of Child Health, University College London, as an Honorary Research Associate and NHS Great Ormond Street Hospital for Children, London, as a Research Fellow. Since 2013, he has been a Research Scientist with the A*STAR Institute for Infocomm Research, Singapore, where he currently serves as the Assistant Head of the Robotics and Autonomous Systems Department. His research interests include robot learning and human–robot interaction.

Shuzhi Sam Ge (S'90-M'92-SM'00-F'06) received the Ph.D. degree from the Imperial College London, London, U.K., in 1993, and the B.Sc. degree from the Beijing University of Aeronautics and Astronautics, Beijing, China, in 1986. He is the Director with the Social Robotics Laboratory of Interactive Digital Media Institute, Singapore, and the Centre for Robotics, Chengdu, China, and a Professor with the Department of Electrical and Computer Engineering, National University of Singapore, Singapore, on leave from the School of Computer Science and Engineering, University of Electronic Science and Technology of China, Chengdu. He has co-authored four books and over 300 international journal and conference papers. His current research interests include social robotics, adaptive control, intelligent systems, and artificial intelligence.

Dr. Ge is Editor-in-Chief of the *International Journal of Social Robotics* (Springer). He has served/been serving as an Associate Editor for a number of flagship journals, including *IEEE Transactions on Automation Control*, *IEEE Transactions on Control Systems Technology*, *IEEE Transactions on Neural Networks* and *Automatica*. He serves as a Book Editor for the Taylor and Francis Automation and Control Engineering Series. He served as the Vice President for Technical Activities, from 2009 to 2010, the Vice President of Membership Activities, from 2011 to 2012, and a member of the Board of Governors, from 2007 to 2009 at the IEEE Control Systems Society. He is a Fellow of the International Federation of Automatic Control, the Institution of Engineering and Technology, and the Society of Automotive Engineering.

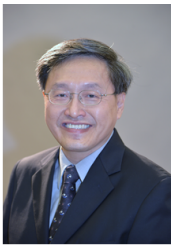

Tong Heng Lee received the B.A. degree with First Class Honours in the Engineering Tripos from Cambridge University, England, in 1980; the M.Engrg. degree from NUS in 1985; and the Ph.D. degree from Yale University in 1987. He is a Professor in the Department of Electrical and Computer Engineering at the National University of Singapore (NUS); and also a Professor in the NUS Graduate School, NUS NGS. He was a Past Vice-President (Research) of NUS.

Dr. Lee's research interests are in the areas of adaptive systems, knowledge-based control, intelligent mechatronics and computational intelligence. He currently holds Associate Editor appointments in the IEEE Transactions in Systems, Man and Cybernetics; Control Engineering Practice (an IFAC journal); and the International Journal of Systems Science (Taylor and Francis, London). In addition, he is the Deputy Editor-in-Chief of IFAC Mechatronics journal.